

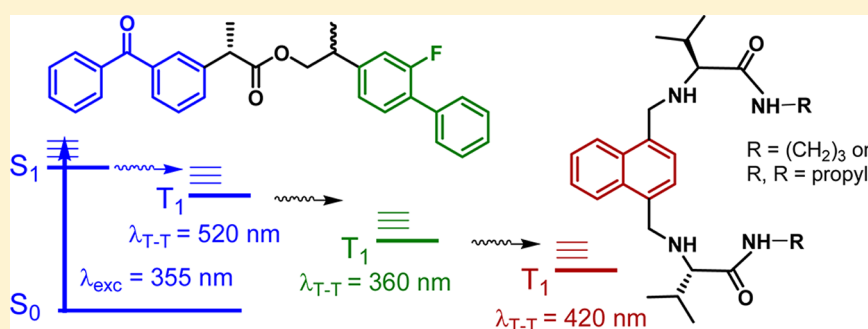
Triplet Excited State Behavior of Naphthalene-Based Pseudopeptides in the Presence of Energy Donors

Paula Bonancía,[†] Laura Vigara,[‡] Francisco Galindo,[‡] Santiago V. Luis,[‡] M. Consuelo Jiménez,^{*,†} and Miguel A. Miranda^{*,†}

[†]Departamento de Química/Instituto de Tecnología Química UPV-CSIC, Universitat Politècnica de Valencia, Camino de Vera s/n, 46071 Valencia, Spain

[‡]Departamento de Química Inorgánica y Orgánica, Universitat Jaume I, Av. Sos Baynat, s/n, 12071 Castellón, Spain

S Supporting Information



ABSTRACT: In this work, the triplet state behavior of naphthalene-based pseudopeptides with amide-based macrocyclic or lateral chain substructures has been investigated in the presence of benzophenone and/or biphenyl, as suitable energy-donating chromophores. Their behavior has been compared with that of 1,4-dimethylnaphthalene as model compound. In all the cases, the triplet–triplet absorption of naphthalene is detected by transient absorption spectroscopy, upon selective excitation of benzophenone at 355 nm. The kinetics of formation and decay of this species is markedly slower in the pseudopeptides, due to retardation of triplet–triplet energy transfer and exciplex formation. Finally, the delayed fluorescence detected in the model naphthalene is absent in the pseudopeptides. The concept can, in principle, be exploited for the study of excited-state interactions in supramolecular systems.

INTRODUCTION

Pseudopeptidic compounds are suitable hosts for a variety of species; this is in the origin of molecular recognition phenomena,^{1–3} which have found application in fields such as medicinal,^{4,5} analytical,⁶ or supramolecular^{7–9} chemistry. In particular, pseudopeptides are synthetic models employed to gain insight into biological processes of high complexity.^{10–12} A powerful strategy in the design of such models could be the incorporation of an active chromophore into the chemical structure of the pseudopeptide, which ultimately would report on the supramolecular interactions with a given guest, through the absorption and emission properties of its excited states.

Concerning the use of photophysical parameters to obtain relevant information on binding interactions, most of the previous work has been done by examining the behavior of singlet excited states using either steady-state or time-resolved fluorescence techniques.¹³ In comparison, the use of triplet excited states as reporters remains almost unexplored,¹⁴ although the laser flash photolysis technique has proven to be a promising tool in such type of investigations.^{15–23}

An essential requirement for an appropriate chromophore to be incorporated into the pseudopeptide structure is that its

main photophysical properties are well-defined and can be easily characterized. For that reason, naphthalene (NPT) is a suitable choice. Thus, fluorescence from the lowest-lying singlet excited state $^1\text{NPT}^*$ ($\phi_F = 0.19–0.21$) is centered at 350 nm (although longer-wavelength emission from NPT excimers has also been reported). After intersystem crossing (ϕ_{ISC} , ca. 0.75), the triplet excited state $^3\text{NPT}^*$ ($E_T = 61$ kcal/mol)²⁴ is reached; its transient absorption can be detected at $\lambda_{max} = 410–430$ nm in the laser flash photolysis (LFP) spectrum.²⁵ Delayed P-type fluorescence in NPT derivatives can also occur, arising from the annihilation of two $^3\text{NPT}^*$ units, to produce again $^1\text{NPT}^*$ through direct irradiation. From this wealth of photophysical information, it can be anticipated that incorporation of the NPT chromophore into a pseudopeptidic framework may provide an efficient tool for the investigation of excited-state interactions with complexed guests.

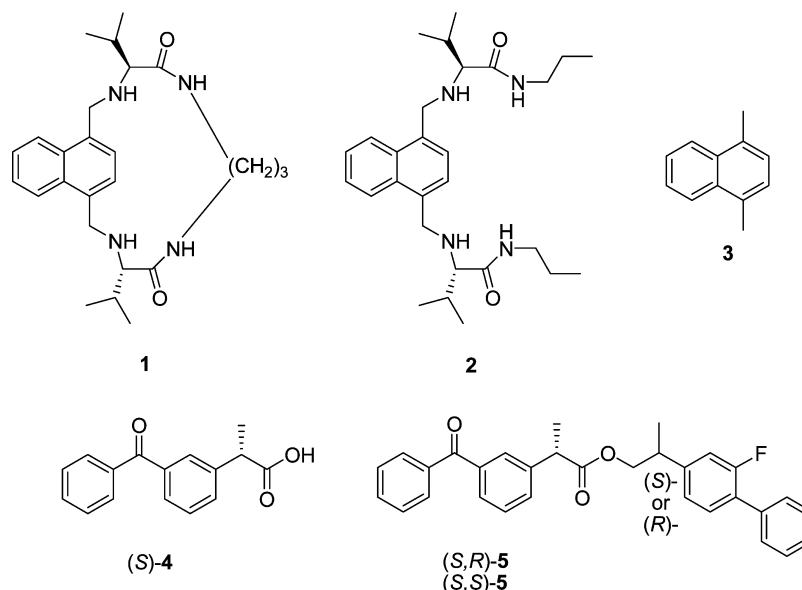
In this context, the fluorescence properties of pseudopeptides containing NPT subunits have already found application for the

Received: May 20, 2012

Revised: August 3, 2012

Published: August 3, 2012

Chart 1



radiometric sensing of N-protected amino acid derivatives.²⁶ However, the potential of the corresponding NPT triplet excited state still remains unexplored. In order to bypass formation of $^1\text{NPT}^*$, benzophenone (BZP) derivatives can be envisaged as triplet photosensitizers, leading exclusively to $^3\text{NPT}^*$. This is based on the possibility of selective excitation of BZP at $\lambda > 320$ nm and to its favorable values of ϕ_{ISC} and E_{T} .

With this background, the objective of this work is to investigate the triplet excited state behavior of naphthalene-based pseudopeptides **1** and **2** in the presence of benzophenone or biphenyl (BPN), using 1,4-dimethylnaphthalene (**3**) for comparison. For the studies in the presence of BZP, (S)-ketoprofen ((S)-**4**) has been selected. In the case of BPN, direct excitation of the chromophore is not possible in the presence of NPT. For this reason, in order to generate selectively $^3\text{BPN}^*$, model dyads **5** containing (R)- or (S)-2-(2-fluorobiphenyl-4-yl)propan-1-ol, ((R)- or (S)-FBPOH), covalently linked to (S)-**4** as the photoexcitable unit seem appropriate. Thus, selective excitation of BZP ($E_{\text{T}} = 69$ kcal mol⁻¹) followed by T–T energy transfer to BPN ($E_{\text{T}} = 65$ kcal mol⁻¹) may in principle lead to population of $^3\text{BPN}^*$ in order to follow the deactivation channels in the presence of **1**–**3**. Thus, the complex behavior of the triplet excited state manifold is expected to reveal interesting features of the pseudopeptides/benzophenone or biphenyl interactions. The chemical structures of **1**–**5** are shown in Chart 1.

EXPERIMENTAL SECTION

Materials and Solvents. (S)-Ketoprofen, (S)- and (R)-flurbiprofen, dicyclohexylcarbodiimide, and 1,4-dimethylaminopyridine were commercially available. Their purity was checked via ^1H nuclear magnetic resonance (NMR) and high-performance liquid chromatography (HPLC) analysis. Reagent or spectroscopic-grade solvents were used without further purification.

General. ^1H NMR spectra were measured in CDCl_3 , using a 300 MHz apparatus; chemical shifts are reported in δ (ppm) values, using tetramethylsilane (TMS) as an internal standard. High-resolution mass spectrometry was performed with a UPLC-MS-MS system at the Instituto de Tecnología Química

UPV-CSIC. Isolation and purification were performed using preparative layer chromatography on silica gel.

Synthesis of Dyads (S,S)-5 and (S,R)-5. Dyads (S,S)-5 and (S,R)-5 were prepared in two steps. First, (S)- or (R)-FBP was reduced. Thus, FBP (1.23 mmol) was dissolved in 12 mL of dry ether at 0 °C; then 5 mL (4.90 mmol) of 1 M LiAlH_4 in ether was added dropwise, and the mixture was heated under reflux for 1 h. The crude was cooled to room temperature and washed with water (3×10 mL). The organic phases were combined, dried over MgSO_4 and evaporated to afford quantitatively (R)- or (S)-2-(2-fluorobiphenyl-4-yl)propan-1-ol ((R)- or (S)-FBPOH), which were used directly in the following reaction without further purification. To a cold solution of (R)- or (S)-FBPOH (0.87 mmol) in ether (25 mL), dicyclohexylcarbodiimide (1.30 mmol) was added portion wise. Then, a solution of (S)-**4** (0.87 mmol) and 4-dimethylaminopyridine (catalytic amounts) in ether (25 mL) was added, and the mixture was stirred for 24 h at room temperature. Brine was added, and the mixture was extracted with ether (3×5 mL). The combined organic layers were washed with water, dried over MgSO_4 , evaporated, and purified using preparative layer chromatography (eluent hexane/ethyl acetate, 75/25 v/v).

Spectroscopic Characterization of (S,S)-5 and (S,R)-5. (S)-2-(2-Fluorobiphenyl-4-yl)propyl (S)-2-(3-benzoylphenyl)propanoate, (S,S)-5. Yield: 42%. ^1H NMR (CDCl_3) (δ , ppm) 1.24 (d, 3H, $J = 7.0$ Hz), 1.50 (d, 3H, $J = 7.2$ Hz), 3.01–3.13 (m, 1H), 3.77 (q, 1H, $J = 7.2$ Hz), 4.14–4.24 (m, 2H), 6.88–6.96 (m, 2H), 7.27–7.78 (m, 15H). ^{13}C NMR (CDCl_3) (δ , ppm) 17.7, 18.2, 38.5, 45.4, 69.3, 114.7 + 115.0, 123.2 + 123.3, 127.0 + 127.1, 127.6, 128.3, 128.4, 128.5, 128.9, 129.0, 129.2, 130.0, 130.6, 131.5, 132.5, 135.6, 137.5, 137.9, 140.7, 144.6 + 144.7, 157.9 + 161.2, 173.8, 196.4. HRMS for $\text{C}_{31}\text{H}_{27}\text{FO}_3$ (MH^+): calcd. 467.2022, found: 467.2017. UV λ_{max} (log ϵ): 200 (4.7), 250 (4.4), 340 (2.1).

(R)-2-(2-Fluorobiphenyl-4-yl)propyl (S)-2-(3-benzoylphenyl)propanoate, (S,R)-5. Yield: 45%. ^1H NMR (CDCl_3) (δ , ppm) 1.23 (d, 3H, $J = 7.0$ Hz), 1.51 (d, 3H, $J = 7.2$ Hz), 3.03–3.13 (m, 1H), 3.78 (q, 1H, $J = 7.2$ Hz), 4.10–4.16 (m, 1H), 4.23–4.31 (m, 1H), 6.89–6.99 (m, 2H), 7.28–7.77 (m, 15H). ^{13}C NMR (CDCl_3) (δ , ppm) 17.7, 18.2, 38.4, 45.4,

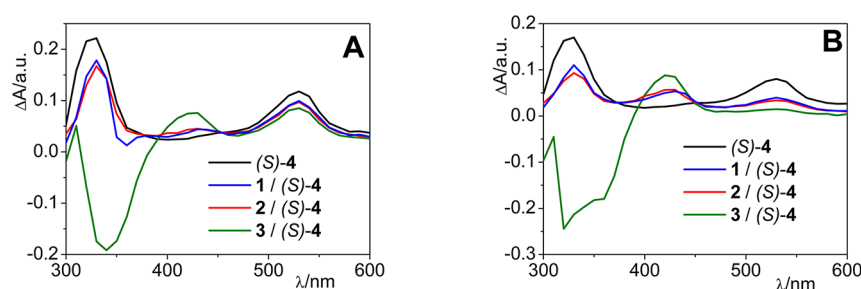


Figure 1. Laser flash photolysis ($\lambda_{exc} = 355$ nm, MeCN, N_2) of (S)-4 at 2.6×10^{-3} M concentration alone (black) or in the presence of 1 (blue), 2 (red), or 3 (green) at 2.6×10^{-4} M concentration. Spectra recorded (A) 0.15 μs or (B) 0.69 μs after the laser pulse.

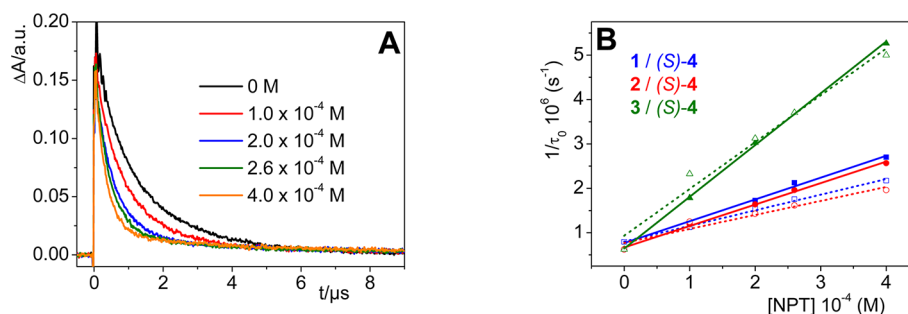


Figure 2. Laser flash photolysis of (S)-4 ($\lambda_{exc} = 355$ nm, 2.6×10^{-3} M, MeCN, N_2) in the presence of increasing amounts of NPT derivatives 1–3. (A) Kinetic traces monitored at 530 nm in the presence of 1. (B) Stern–Volmer plots for $^3BZP^*$ quenching by 1 (blue), 2 (red), and 3 (green) in the absence (solid lines) and in the presence of 0.6 M HOAc (dotted lines).

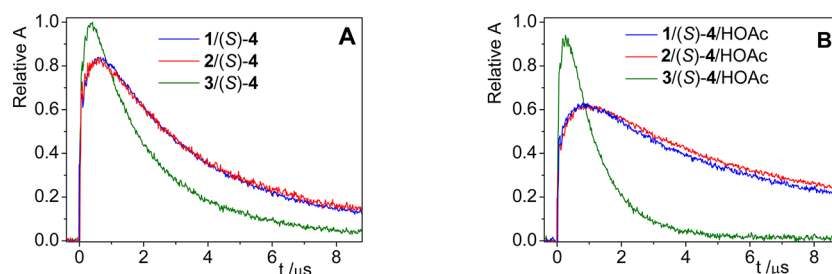


Figure 3. Laser flash photolysis ($\lambda_{exc} = 355$ nm, MeCN, N_2) of (S)-4 2.6×10^{-3} M in the presence of 1 (blue), 2 (red), or 3 (green) at 2.6×10^{-4} M concentration. Decay traces monitored at 430 nm; the maximum value of the absorbance (1.0) corresponds to the system 3/(S)-4. (A) In the absence of HOAc. (B) In the presence of HOAc 0.6 M.

69.3, 114.7 + 115.0, 123.2 + 123.3, 127.0 + 127.1, 127.6, 128.3, 128.4, 128.7, 128.9, 129.0, 129.2, 130.0, 130.6, 131.5, 132.5, 135.6, 137.5, 137.8, 140.7, 144.6 + 144.7, 158.0 + 161.3, 173.9, 196.4. HRMS for $C_{31}H_{27}FO_3$ (MH^+): calcd. 467.2022, found: 467.2020. UV λ_{max} (log ϵ): 200 (4.7), 250 (4.4), 340 (2.1).

Laser Flash Photolysis Experiments. Laser flash photolysis (LFP) experiments were performed by using a Q-switched Nd:YAG laser (Quantel Brilliant, 355 nm, 20 mJ per pulse, 5 ns fwhm) coupled to a mLFP-111 Luzchem miniaturized equipment. This transient absorption spectrometer includes a ceramic xenon light source, 125 mm monochromator, Tektronix 9-bit digitizer TDS-3000 series with 300 MHz bandwidth, compact photomultiplier and power supply, cell holder and fiber optic connectors, fiber optic sensor for laser-sensing pretrigger signal, computer interfaces, and a software package developed in the LabVIEW environment from National Instruments. The LFP equipment supplies 5 V trigger pulses with programmable frequency and delay. The rise time of the detector/digitizer is ~ 3 ns up to 300 MHz (2.5 GHz sampling). The monitoring beam is provided by a ceramic xenon lamp and delivered through fiber optic cables. The laser

pulse is probed by a fiber that synchronizes the LFP system with the digitizer operating in the pretrigger mode. All transient spectra were recorded using 10 mm \times 10 mm quartz cells with a capacity of 4 mL and were bubbled for 30 min with N_2 before signal acquisition. The absorbance of the samples was 0.2 at the laser excitation wavelength (355 nm).

RESULTS AND DISCUSSION

Pseudopeptidic naphthalene derivatives 1 and 2 belong to a family of molecules employed as model compounds in supramolecular chemistry.^{6,13,14,26–30} The synthesis of 1 and 2 has been reported elsewhere³¹ and is based on coupling of 1,4-bis(bromomethylnaphthalene) with valine; however, while 1 presents a macrocyclic structure, 2 conserves open chains at both sides of NPT. Together with 1 and 2, the behavior of 1,4-dimethylnaphthalene (3) was also studied as the simplest model for comparison.

The UV–vis absorption spectrum of (S)-4 (MeCN, 1×10^{-3} M) exhibited the characteristic $S_0 \rightarrow S_1$ band (320–390 nm). In the presence of increasing amounts of 1–3 (from 1×10^{-4} to 4×10^{-4} M), this spectral region did not show any noticeable

change, indicating that selective excitation of the benzophenone chromophore is possible at long wavelengths (Figure S1 in the Supporting Information). The transient absorption spectrum ($\lambda_{\text{exc}} = 355 \text{ nm}$, N_2) of pure (S)-4 at $2.6 \times 10^{-3} \text{ M}$ concentration displayed the typical $^3\text{BZP}^*$ band peaking at 530 nm ($\tau_{\text{T}} = 1.6 \mu\text{s}$). After addition of 1, 2, or 3 (in the absence or presence of HOAc), new spectra were obtained (Figure 1A,B and Figure S2A–F in the Supporting Information).

It became clear that $^3\text{BZP}^*$ is efficiently quenched through a T–T energy transfer mechanism, leading to $^3\text{NPT}^*$ (band centered at $\lambda_{\text{max}} = 430 \text{ nm}$). As expected, the process was faster at higher naphthalene concentrations (Figure 2A,B and Figure S3A–F in the Supporting Information). Interestingly, the growth and decay of $^3\text{NPT}^*$ were clearly slower for the pseudopeptides than for model 3 (see Figure 3). The following observations apply to (S)-4/1–3 mixtures at 10:1 molar ratio, although the trend was similar within a broader range (26:1 to 6:1). Thus, $^3\text{1}^*$ and $^3\text{2}^*$ were formed relatively slowly ($480 \text{ ns} < \tau_{\text{growth}} < 620 \text{ ns}$) in comparison to $^3\text{3}^*$ ($\tau_{\text{growth}} = 271 \text{ ns}$), as observed from the initial rise of the trace monitored at $\lambda = 430 \text{ nm}$. Besides, in acidic medium the maximum was reached for pseudopeptides ca. 100 ns later than in the case of 3.

From the slope of the corresponding Stern–Volmer plots (Figure 2B), it was possible to obtain the corresponding k_{Q} values (Table 1); they indicated that quenching is similar for

Table 1. Relevant Photophysical Parameters for Triplet Excited States of (S)-4/1–3 Systems

	conditions ^a	$k_{\text{Q}}/10^{10} (\text{M}^{-1} \text{s}^{-1})^b$	$\tau_{\text{growth}} (\text{ns})^c$	rel A (%) ^d	$\tau_{\text{T}} (\mu\text{s})^e$
1	A	0.49 ± 0.02	477 ± 4	84	3.25 ± 0.02
	B	0.34 ± 0.01	571 ± 5	63	6.05 ± 0.03
2	A	0.48 ± 0.01	513 ± 4	84	3.15 ± 0.02
	B	0.32 ± 0.04	616 ± 4	63	6.53 ± 0.03
3	A	1.16 ± 0.02	271 ± 3	100	1.79 ± 0.01
	B	1.05 ± 0.01	271 ± 2	94	1.11 ± 0.02

^aA = MeCN, B = MeCN, HOAc 0.6 M. ^bQuenching constant for $^3\text{4}^*$ ($\lambda_{\text{exc}} = 355 \text{ nm}$, $2.6 \times 10^{-3} \text{ M}$) monitored at 530 nm in the presence of increasing amounts of NPT derivatives (from 1×10^{-4} to $4 \times 10^{-4} \text{ M}$). ^cRise of the $^3\text{NPT}^*$ signal, at 430 nm . ^dMaximum of the signal at $\lambda = 430 \text{ nm}$ for each NPT/BZP system (10:1 molar ratio), relative to 3/(S)-4 in the absence of HOAc, given as percentage. ^eTriplet lifetime of $^3\text{NPT}^*$, from the trace at 430 nm .

both pseudopeptides and faster for 3. The same trend was observed in acidic medium, although the processes took place at longer time scales.

Furthermore, comparison of the maximum absorbance values at 430 nm indicated that T–T energy transfer is more efficient in nonacidic medium, and that the amount of $^3\text{3}^*$ is higher than those of $^3\text{1}^*$ and $^3\text{2}^*$. This is in good agreement with the corresponding values of the rate constants found for quenching of the excited state precursor ($^3\text{4}^*$). These data could indicate that the geometry of approach between donor BZP and acceptor NPT is actually influenced by the pseudopeptidic architecture surrounding the polyaromatic chromophore in 1 and 2. Concerning the $^3\text{NPT}^*$ decay dynamics (linked to formation of a triplet exciplex between $^3\text{NPT}^*$ and BZP), the values of τ_{T} were almost coincident for $^3\text{1}^*$ and $^3\text{2}^*$, while $^3\text{3}^*$ was shorter-lived; i.e., the decay of the complex formed by BZP and $^3\text{1}^*$ or $^3\text{2}^*$ is retarded by the presence of the pseudopeptidic framework; this effect was more pronounced in acidic medium.

Relevant data are summarized in Table 1. In addition, the most remarkable difference found between the transient absorption spectra of pseudopeptides 1 and 2 and the model compound 3 was the absence of the negative band centered at 340 nm in the former. This signal can be attributed to delayed fluorescence from $^1\text{NPT}^*$, which arises through annihilation of the $^3\text{NPT}^*$ precursor and occurs in the microsecond time scale. A full LFP characterization of P-type delayed fluorescence in BZP/NPT systems has been recently published.³² Again, the absence of appreciable T–T annihilation could be due to the shielding effect caused by the pseudopeptidic moieties surrounding the naphthalene chromophore in the case of 1 and 2.

In order to investigate the triplet excited state interactions between biphenyl and pseudopeptides 1 and 2, (S)-4 was covalently linked to (S)- or (R)-2-(2-fluorobiphenyl-4-yl)-propan-1-ol (obtained by reduction of flurbiprofen).³³ In order to detect possible stereodifferentiation in the excited-state interactions, dyads (S,S)- and (S,R)-5 were prepared. Their absorption spectra are also shown in Figure S6 (Supporting Information). Excitation of these dyads at $\lambda > 330 \text{ nm}$ should initially result in generation of $^3\text{BZP}^*$; however, after fast intramolecular T–T energy transfer $^3\text{BPN}^*$ would be selectively populated. The transient absorption spectra of (S,S)- and (S,R)-5 obtained after LFP at $\lambda_{\text{exc}} = 355 \text{ nm}$ are shown in Figure S7 (Supporting Information); their most remarkable feature is the presence of an intense band centered at 360 nm due to $^3\text{BPN}^*$,³⁴ together with a residual trace of $^3\text{BZP}^*$ at longer wavelengths ($500\text{--}550 \text{ nm}$). In the presence of 1–3 (Figure 4), formation of $^3\text{BPN}^*$ was still detected at shorter lifetimes, although at longer time scales the spectral shape changed, and the typical $^3\text{NPT}^*$ band emerged at $\lambda = 430 \text{ nm}$. The kinetic behavior was different for pseudopeptides 1 and 2

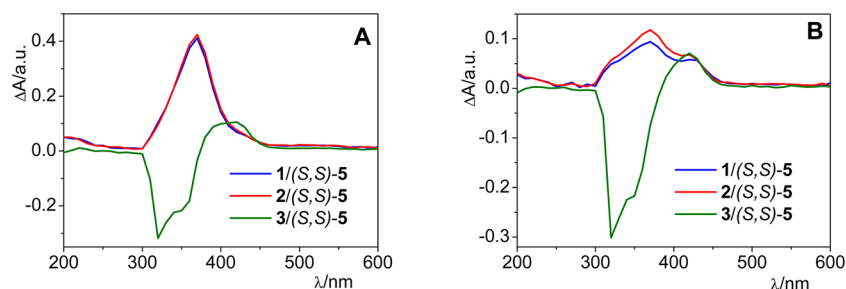


Figure 4. Laser flash photolysis ($\lambda_{\text{exc}} = 355 \text{ nm}$, MeCN, N_2 , $2.6 \times 10^{-3} \text{ M}$) of (S,S)-5 in the presence of 1 (blue), 2 (red), or 3 (green), at $2.6 \times 10^{-4} \text{ M}$ concentration. Spectra recorded at different time windows: (A) $0.20 \mu\text{s}$; (B) $1.00 \mu\text{s}$.

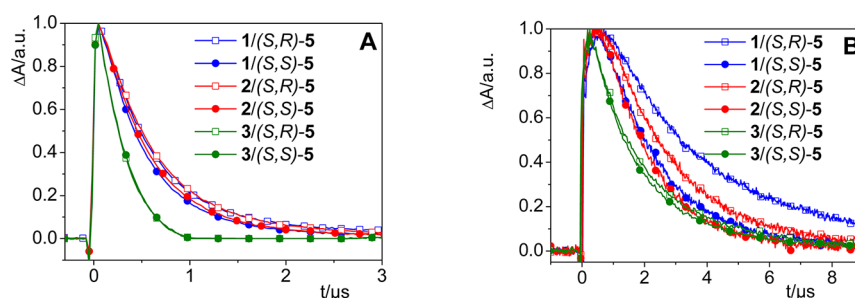


Figure 5. Laser flash photolysis ($\lambda_{\text{exc}} = 355$ nm, MeCN, N_2) of (S,S)-5 and (S,R)-5 at 2.6×10^{-3} M concentration, in the presence of 1, 2, or 3, 2.6×10^{-4} M. Normalized decays monitored at (A) 360 nm and (B) 430 nm.

and for the model compound 3 (Figure 5). Thus, in the spectra of (S,S)-5 in the presence of 1 and 2, both $^3\text{BPN}^*$ and $^3\text{NPT}^*$ contributions are observable in the second time window (1 μs after the laser pulse). However, only $^3\text{NPT}^*$ was detected under the same conditions in the presence of 3; remarkably, the negative band peaking at 330 nm, due to $^1\text{NPT}^*$ delayed fluorescence was also clearly visible in this case. The behavior of (S,R)-5 was similar; additional information is provided in Figures S8 and S9 of the Supporting Information.

The decays at 360 nm ($^3\text{BPN}^*$) and 430 nm ($^3\text{NPT}^*$) for the different combinations of (S,S)-5 and (S,R)-5 in the presence of 1–3 are shown in Figure 5. At both wavelengths, the decay was slower for pseudopeptides 1 and 2 than for the model compound 3. Besides, a significant stereodifferentiation was found for the kinetic traces of the $^3\text{NPT}^*$ species, with (S,R)-5 decaying consistently slower than its stereoisomer (S,S)-5. Notably, in the case of the open-chain derivative 2, the $^3\text{NPT}^*$ lifetime is significantly longer for (S,R)-5 than for (S,S)-5 (2.50 versus 1.89 μs). Moreover, for macrocycle 1, the more preorganized host, stereodifferentiation was even larger (triplet lifetimes 3.52 versus 1.92 μs). This supports the formation of an excited-state complex between donor 5 and chiral hosts 1 and 2, and is in agreement with the fact that achiral host 3 does not discriminate between diastereomeric guests (S,S)-5 and (S,R)-5.

The biphenyl and naphthalene triplet lifetimes are presented in Table 2. Triplet–triplet energy transfer from BZP to BPN

Table 2. Triplet Lifetimes of BPN and NPT in NPT/BZP–BPN Systems

NPT derivative	dyad	$\tau(^3\text{BPN}^*)/\mu\text{s}$	$\tau(^3\text{NPT}^*)/\mu\text{s}$
none	(S,S)-5	1.45 ± 0.01	–
none	(S,R)-5	2.20 ± 0.01	–
1	(S,S)-5	0.52 ± 0.01	1.92 ± 0.02
1	(S,R)-5	0.62 ± 0.01	3.52 ± 0.03
2	(S,S)-5	0.59 ± 0.01	1.89 ± 0.05
2	(S,R)-5	0.66 ± 0.01	2.50 ± 0.06
3	(S,S)-5	0.30 ± 0.01	1.75 ± 0.01
3	(S,R)-5	0.30 ± 0.01	1.65 ± 0.01

was a very efficient process, both in the absence and in the presence of NPT derivatives. Thus, the band of $^3\text{BZP}^*$ was almost negligible already at the early time windows, and its lifetimes could not be determined accurately.

CONCLUSIONS

In summary, the triplet excited state of the NPT chromophore in 1 and 2 is an appropriate reporter for the interactions

between these pseudopeptides and mono- or bichromophoric systems containing triplet energy-donating moieties such as BZP and/or BPN. The presence of the macrocyclic or lateral chain substructures of 1 and 2 has a marked influence on the dynamics of the triplet manifold, retarding all the triplet–triplet energy-transfer processes, as well as $^3\text{NPT}^*$ deactivation via exciplex formation. Finally, the delayed fluorescence clearly detected in the model compound 3, as a result of the triplet–triplet annihilation, is absent in the pseudopeptides. This concept can, in principle, be exploited for the study of the excited-state interaction in supramolecular systems.

ASSOCIATED CONTENT

Supporting Information

Absorption spectra, additional laser flash photolysis spectra and spectroscopic characterization of dyads (S,S)-5 and (S,R)-5. This material is available free of charge via the Internet at <http://pubs.acs.org>.

AUTHOR INFORMATION

Corresponding Author

*E-mail: mcjimene@qim.upv.es (M.C.J.); mmiranda@qim.upv.es (M.A.M.).

Notes

The authors declare no competing financial interest.

ACKNOWLEDGMENTS

Financial support from the MICINN (Grants CTQ-2010-14882, CTQ2009-14366-C02-01 and FPI contract to P.B.), the Generalitat Valenciana (Prometeo 2008/090), the UPV (PAID 05-11 Program, ref 2766), and Fundació Caixa Castelló-UJI (P1 1B-2009-59) is gratefully acknowledged.

REFERENCES

- (1) Lehn, J.-M. *Supramolecular Chemistry: Concepts and Perspectives*; Wiley-VCH: Weinheim, Germany, 1995.
- (2) Cavalli, S.; Albericio, F.; Kros, A. *Chem. Soc. Rev.* **2010**, 39, 241–263.
- (3) Uhlenheuer, D. A.; Petkau, K.; Brunsveld, L. *Chem. Soc. Rev.* **2010**, 39, 2817–2826.
- (4) Loo, Y.; Zhang, S.; Hauser, C. A. E. *Biotechnol. Adv.* **2012**, 30, 593–603.
- (5) Neffe, T.; Bilanz, M.; Grüneberg, I.; Meyer, B. *J. Med. Chem.* **2007**, 50, 3482–3488.
- (6) Laurencin, M.; Legrand, B.; Duval, E.; Henry, J.; Baudy-Floc'h, M.; Zatylny-Gaudin, C.; Bondon, A. *J. Med. Chem.* **2012**, 55, 2025–2034.
- (7) Galindo, F.; Burguete, M. I.; Vigara, L.; Luis, S. V.; Kabir, N.; Gavrilovic, J.; Russell, D. A. *Angew. Chem., Int. Ed.* **2005**, 44, 6504–6508.

- (7) Clark, J. L.; Peinado, J.; Stezowski, J. J.; Vold, R. L.; Huang, Y.; Hoatson, G. L. *J. Phys. Chem. B* **2006**, *110*, 26375–26387.
- (8) Angelici, G.; Castellucci, N.; Falini, G.; Huster, D.; Monari, M.; Tomasini, C. *Cryst. Growth Des.* **2010**, *10*, 923–929.
- (9) Angelici, G.; Falini, G.; Hofmann, H.-J.; Huster, D.; Monari, M.; Tomasini, C. *Angew. Chem., Int. Ed.* **2008**, *47*, 8075–8078.
- (10) Eichler, J. *Curr. Opin. Chem. Biol.* **2008**, *12*, 707–713.
- (11) Robinson, J. A. *Acc. Chem. Res.* **2008**, *41*, 1278–1288.
- (12) Nielsen, P. E. *Pseudopeptides in Drug Discovery*; Wiley-VCH: Weinheim, Germany, 2004.
- (13) Galindo, F.; Becerril, J.; Burguete, M. I.; Luis, S. V.; Vigar, L. *Tetrahedron Lett.* **2004**, *45*, 1659–1662.
- (14) Salom-Roig, X. J.; Martínez, J.; Burguete, M. I.; Galindo, F.; Luis, S. V.; Miranda, M. A.; Morant-Miñana, M. C.; Pérez-Prieto, J. *Tetrahedron Lett.* **2009**, *50*, 4859–4862.
- (15) Vayá, I.; Bueno, C. J.; Jiménez, M. C.; Miranda, M. A. *ChemMedChem* **2006**, *1*, 1015–1020.
- (16) Jiménez, M. C.; Miranda, M. A.; Vayá, I. *J. Am. Chem. Soc.* **2005**, *127*, 10134–10135.
- (17) Vayá, I.; Jiménez, M. C.; Miranda, M. A. *J. Phys. Chem. B* **2008**, *112*, 2694–2699.
- (18) Lhiaubet-Vallet, V.; Miranda, M. A.; Boscá, F. *J. Phys. Chem. B* **2007**, *111*, 423–431.
- (19) Lhiaubet-Vallet, V.; Sarabia, Z.; Boscá, F.; Miranda, M. A. *J. Am. Chem. Soc.* **2004**, *126*, 9538–9539.
- (20) Vayá, I.; Bueno, C. J.; Jiménez, M. C.; Miranda, M. A. *Chem.—Eur. J.* **2008**, *14*, 11284–11287.
- (21) Bueno, C. J.; Jiménez, M. C.; Miranda, M. A. *J. Phys. Chem. B* **2009**, *113*, 6861–6865.
- (22) Pérez-Ruiz, R.; Bueno, C. J.; Jiménez, M. C.; Miranda, M. A. *J. Phys. Chem. Lett.* **2010**, *1*, 829–833.
- (23) Pérez-Ruiz, R.; Alonso, R.; Nuin, E.; Andreu, I.; Jiménez, M. C.; Miranda, M. A. *J. Phys. Chem. B* **2011**, *115*, 4460–4468.
- (24) Murov, S. L.; Carmichael, I.; Hug, G. L. *Handbook of Photochemistry*; Marcel Dekker: New York, 1993.
- (25) Carmichael, I.; Hug, G. L. *J. Phys. Chem. Ref. Data* **1986**, *15*, 1–250.
- (26) Alfonso, I.; Burguete, M. I.; Galindo, F.; Luis, S. V.; Vigar, L. *J. Org. Chem.* **2009**, *74*, 6130–6142.
- (27) Burguete, M. I.; Galindo, F.; Gavara, R.; Izquierdo, M. A.; Lima, J. C.; Luis, S. V.; Parola, A. J.; Pina, F. *Langmuir* **2008**, *24*, 9795–9803.
- (28) Burguete, M. I.; Galindo, F.; Izquierdo, M. A.; O'Connor, J.-E.; Herrera, G.; Luis, S. V.; Vigar, L. *Eur. J. Org. Chem.* **2010**, 5967–5979.
- (29) Rubio, J.; Izquierdo, M. A.; Burguete, M. I.; Galindo, F.; Luis, S. V. *Nanoscale* **2011**, *3*, 3613–3615.
- (30) Martí-Centelles, V.; Burguete, M. I.; Galindo, F.; Izquierdo, M. A.; Kumar, D. K.; White, A. J. P.; Luis, S. V.; Vilar, R. *J. Org. Chem.* **2012**, *77*, 490–500.
- (31) Burguete, M. I.; Galindo, F.; Izquierdo, M. A.; Luis, S. V.; Vigar, L. *Tetrahedron* **2007**, *63*, 9493–9501.
- (32) Bonancía, P.; Jiménez, M. C.; Miranda, M. A. *Chem. Phys. Lett.* **2011**, *515*, 194–196.
- (33) Asíns-Fabra, B.; Andreu, I.; Jiménez, M. C.; Miranda, M. A. *J. Photochem. Photobiol. A: Chem.* **2009**, *207*, 52–57.
- (34) Jiménez, M. C.; Miranda, M. A.; Tormos, R.; Vayá, I. *Photochem. Photobiol. Sci.* **2004**, *3*, 1038–1041.